

## Search for lepton-flavor-violating $\tau$ decay and lepton-number-violation $B$ decay at Belle

---

**K.Hayasaka**<sup>\*†</sup>

*Nagoya University*

*E-mail: hayasaka@hepl.phys.nagoya-u.ac.jp*

We report on the recent results of searches for lepton-flavor-violating  $\tau$  decays as well as lepton-number-violating  $B$  decays with the world-highest data samples accumulated at the Belle.

*35th International Conference of High Energy Physics - ICHEP2010,*

*July 22-28, 2010*

*Paris France*

---

<sup>\*</sup>Speaker.

<sup>†</sup>the Belle collaboration

## 1. Introduction

An observation of the lepton-flavor-violating (LFV) or the lepton-number-violating (LNV) processes is a clear signature of the existence for physics beyond the standard model (BSM) since they are forbidden in the standard model (SM). Among various LFV processes, some LFV decays of tau lepton are expected to be enhanced by several kinds of BSM, especially, models with supersymmetry. One of the most frequently discussed is  $\tau^- \rightarrow \mu^- \gamma$  decay. But, in some models, such as the non-universal Higgs mass model, the constrained minimal supersymmetric SM and so on, among the  $\tau$  LFV decays,  $\tau^- \rightarrow \mu^- \eta$  or  $\tau^- \rightarrow \mu^- \rho^0$  will be enhanced. [1] In this talk, we report the recent result of a search for  $\tau^- \rightarrow \ell^- M^0$  ( $\ell = e, \mu$ ,  $M^0 = \pi^0, \eta, \eta', \rho^0, K^{*0}, \bar{K}^{*0}, \omega$  and  $\phi$ ) with the world largest data sample accumulated at Belle. On the other hand, some LNV decays are possible when the neutrino is the Majorana type spinor. Here, we show the first result of search for  $B^+ \rightarrow D^- \ell^+ \ell^+$  at Belle.

## 2. $\tau \rightarrow \ell M^0$ ( $\ell = e, \mu$ , $M^0 = \pi^0, \eta, \eta', \rho^0, K^{*0}, \bar{K}^{*0}, \omega$ and $\phi$ )

### 2.1 Analysis Method

In the  $\tau$  LFV analysis, in order to evaluate the number of signal events, two independent variables are defined, that are signal-reconstructed mass and energy in the center-of-mass (CM) frame from energies and momenta for the signal  $\tau$  daughters. In the  $\tau \rightarrow \mu \eta$  case, they are defined as  $M_{\mu\eta} = \sqrt{E_{\mu\eta}^2 - P_{\mu\eta}^2}$ ,  $\Delta E = E_{\mu\eta}^{\text{CM}} - E_{\text{beam}}^{\text{CM}}$ , where  $E_{\mu\eta}$  ( $P_{\mu\eta}$ ) is a sum of the energies (a magnitude of a vector sum of the momenta) for  $\mu$  and  $\eta$ , the superscript CM indicates that the variable is defined in the CM frame and  $E_{\text{beam}}^{\text{CM}}$  means the initial beam energy in the CM frame. Principally,  $M_{\mu\eta}$  and  $\Delta E$  should be  $m_\tau$  ( $\sim 1.78 \text{ GeV}/c^2$ ) and 0 (GeV), respectively, for signal events while  $M_{\mu\eta}$  and  $\Delta E$  will smoothly vary without any special structure in the background (BG) events. Due to a finite resolution, the signal events are distributed around  $M_{\mu\eta} \sim m_\tau$  and  $\Delta E \sim 0$  (GeV). Taking into account the resolution, we set the elliptic signal region. Finally, we evaluate the number of signal events in the signal region. When the number of the observed events is consistent to that of the expected BG events, the upper limit for the number of the signal events is evaluated by Feldman-Cousins method. [2] To avoid any bias, we perform the blind analysis: Before fixing the selection criteria and the evaluation for the systematic uncertainties, we cover the data events in the signal region.

### 2.2 $\tau \rightarrow \ell P^0$ ( $\ell = e, \mu$ , $P^0 = \pi^0, \eta, \eta'$ )

We perform a new search for the  $\tau$  decay into a lepton ( $e$  or  $\mu$ ) and a neutral pseudoscalar ( $\pi^0, \eta$  or  $\eta'$ ) with a  $901 \text{ fb}^{-1}$  data sample. A neutral pion is reconstructed from 2 photons while an  $\eta$  ( $\eta'$ ) is reconstructed from  $\gamma\gamma$  ( $\rho^0\gamma$ ) as well as  $\pi^+\pi^-\pi^0$  ( $\pi^+\pi^-\eta$ ) to increase the detection efficiency. When the neutral pseudoscalars are reconstructed, their four-momentum is evaluated by a mass-constrained fit to obtain a better resolution for the signal region. Because we have modified the selection criteria applied to the previous analysis, we obtain an about 1.5 times better detection efficiency while the similar background level is kept. As a result, we observe one event in the  $\tau \rightarrow e\eta$  ( $\rightarrow \gamma\gamma$ ) mode while no events are found in other modes as shown in Fig. 1. Since these results are consistent with the background estimation, we set upper limits on the following branching

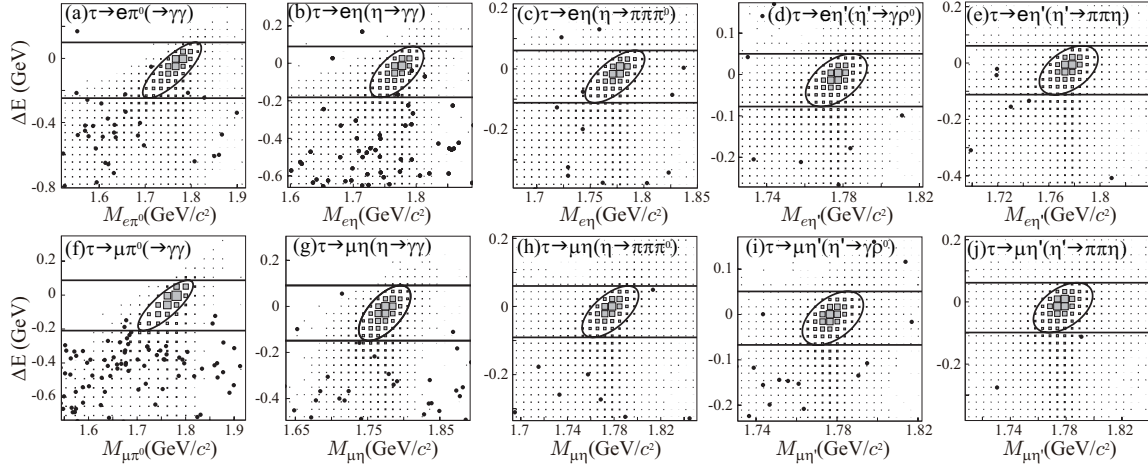


**Figure 1:** Resulting 2D plots for  $\tau \rightarrow e\pi^0$  (a),  $e\eta(\rightarrow \gamma\gamma)$  (b),  $e\eta(\rightarrow \pi\pi\pi^0)$  (c),  $e\eta'(\rightarrow \gamma\rho^0(\rightarrow \pi\pi))$  (d),  $e\eta'(\rightarrow \pi\pi\eta(\rightarrow \gamma\gamma))$  (e),  $\mu\pi^0$  (f),  $\mu\eta(\rightarrow \gamma\gamma)$  (g),  $\mu\eta(\rightarrow \pi\pi\pi^0)$  (h),  $\mu\eta'(\rightarrow \gamma\rho^0(\rightarrow \pi\pi))$  (i) and  $\mu\eta'(\rightarrow \pi\pi\eta(\rightarrow \gamma\gamma))$  (j), on the  $M_{\ell P^0} - \Delta E$  plane. Here, black dots (shaded boxes) express the data (signal MC), the region bounded by two lines is defined as a  $3\sigma$  band for the BG estimation and the elliptic region is the signal one which corresponds to  $3\sigma$  in each plot. One event is found in the signal region for  $\tau \rightarrow e\eta$  while no events appear in any other modes.

fractions:  $\mathcal{B}(\tau^- \rightarrow e^- \pi^0) < 2.7 \times 10^{-8}$ ,  $\mathcal{B}(\tau^- \rightarrow \mu^- \pi^0) < 2.2 \times 10^{-8}$ ,  $\mathcal{B}(\tau^- \rightarrow e^- \eta) < 4.4 \times 10^{-8}$ ,  $\mathcal{B}(\tau^- \rightarrow \mu^- \eta) < 2.3 \times 10^{-8}$ ,  $\mathcal{B}(\tau^- \rightarrow e^- \eta') < 3.6 \times 10^{-8}$  and  $\mathcal{B}(\tau^- \rightarrow \mu^- \eta') < 3.8 \times 10^{-8}$ , at the 90% confidence level.

### 2.3 $\tau \rightarrow \ell V^0$ ( $\ell = e, \mu, V^0 = \rho^0, K^{*0}, \bar{K}^{*0}, \omega, \phi$ )

Similarly to  $\tau^- \rightarrow \ell^- P^0$ , we update our results of the search for  $\tau^- \rightarrow \ell^- V^0$ , where  $\ell = e, \mu$ ,  $V^0 = \rho^0, K^{*0}, \bar{K}^{*0}, \omega, \phi$  with an  $854 \text{ fb}^{-1}$  data sample. By performing a detailed background study, we obtain a 1.2 times better efficiency in average with keeping similar level backgrounds. Finally,

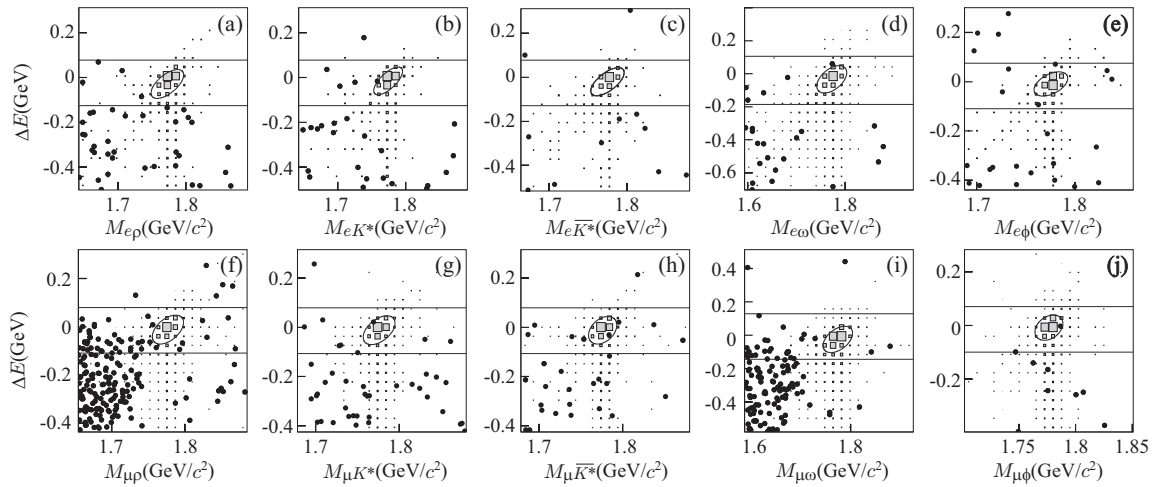


**Figure 2:** Resulting 2D plots for  $\tau \rightarrow e\rho^0$  (a),  $eK^{*0}$  (b),  $e\bar{K}^{*0}$  (c),  $e\omega$  (d),  $e\phi$  (e),  $\mu\rho^0$  (f),  $\mu K^{*0}$  (g),  $\mu\bar{K}^{*0}$  (h),  $\mu\omega$  (i) and  $\mu\phi$  (j) on the  $M_{\ell V^0} - \Delta E$  plane. Here, black dots (shaded boxes) express the data (signal MC), the region bounded by two lines is defined as a  $5\sigma$  band for the BG estimation and the elliptic region is the signal one which corresponds to  $3\sigma$  in each plot. One event is found in the signal region for  $\tau \rightarrow \mu K^{*0}$ ,  $\mu\bar{K}^{*0}$  and  $\mu\phi$  while no events appear in any other modes.

one event is found in the signal region for  $\tau^- \rightarrow \mu^- K^{*0}$ ,  $\mu^- \bar{K}^{*0}$  and  $\mu^- \phi$  while no events appear in any other modes. They are consistent with the expected number of the backgrounds. Consequently, we set the 90% confidence level upper limits on the branching fractions:  $\mathcal{B}(\tau^- \rightarrow e^- \rho^0) < 1.8 \times 10^{-8}$ ,  $\mathcal{B}(\tau^- \rightarrow e^- K^{*0}) < 3.2 \times 10^{-8}$ ,  $\mathcal{B}(\tau^- \rightarrow e^- \bar{K}^{*0}) < 3.4 \times 10^{-8}$ ,  $\mathcal{B}(\tau^- \rightarrow e^- \omega) < 4.8 \times 10^{-8}$ ,  $\mathcal{B}(\tau^- \rightarrow e^- \phi) < 3.1 \times 10^{-8}$ ,  $\mathcal{B}(\tau^- \rightarrow \mu^- \rho^0) < 1.2 \times 10^{-8}$ ,  $\mathcal{B}(\tau^- \rightarrow \mu^- K^{*0}) < 7.2 \times 10^{-8}$ ,  $\mathcal{B}(\tau^- \rightarrow \mu^- \bar{K}^{*0}) < 7.0 \times 10^{-8}$ ,  $\mathcal{B}(\tau^- \rightarrow \mu^- \omega) < 4.7 \times 10^{-8}$ ,  $\mathcal{B}(\tau^- \rightarrow \mu^- \phi) < 8.4 \times 10^{-8}$ .

### 3. $B^+ \rightarrow \ell^+ \ell'^+ D^-$ ( $\ell, \ell' = e, \mu$ )

If the neutrino is a Majorana-type spinor, a  $B^+ \rightarrow \ell^+ \ell'^+ h^-$  decay is possible, where  $\ell, \ell' = e, \mu$ ,  $h = \pi, K, \rho, K^*, D, \dots$  [3]. Due to the size of CKM matrix,  $B^+ \rightarrow \ell^+ \ell'^+ D^-$  is expected to have the largest branching fraction among them. But this mode has never been measured yet. Using a  $7.7 \times 10^8 B^+ B^-$  data sample, we perform a first search. Similarly to the  $\tau$  LFV case, we define  $M_{bc}$  and  $\Delta E$ , where they are reconstructed from  $\ell^+$ ,  $\ell'^+$  and  $D^-$ , but the total energy is set to the initial beam energy. In order to evaluate the number of signal events, the signal box is defined as  $5.27 \text{ (GeV}/c^2) < M_{bc} < 5.29 \text{ (GeV}/c^2)$  and  $-0.035 \text{ (GeV)} < \Delta E < 0.035 \text{ (GeV)}$  for  $B^+ \rightarrow \mu^+ \mu^+ D^-$ , or  $-0.055 \text{ (GeV)} < \Delta E < 0.035 \text{ (GeV)}$  for others, because the distribution for the electron energy has a small tail on the lower side. After the selection, we found no events in the signal box for all modes. Finally, we set the 90% confidence level upper limits on the branching fractions:  $\mathcal{B}(B^+ \rightarrow e^+ e^+ D^-) < 2.7 \times 10^{-6}$ ,  $\mathcal{B}(B^+ \rightarrow e^+ \mu^+ D^-) < 1.9 \times 10^{-6}$ ,  $\mathcal{B}(B^+ \rightarrow \mu^+ \mu^+ D^-) < 1.1 \times 10^{-6}$ .

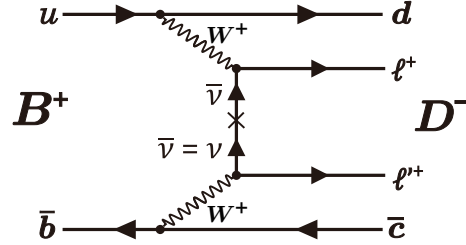


**Figure 3:** Decay process for  $B^+ \rightarrow \ell^+ \ell'^+ D^-$ . When a neutrino is a Majorana spinor, the neutrinos can connect as an inner line in the process.

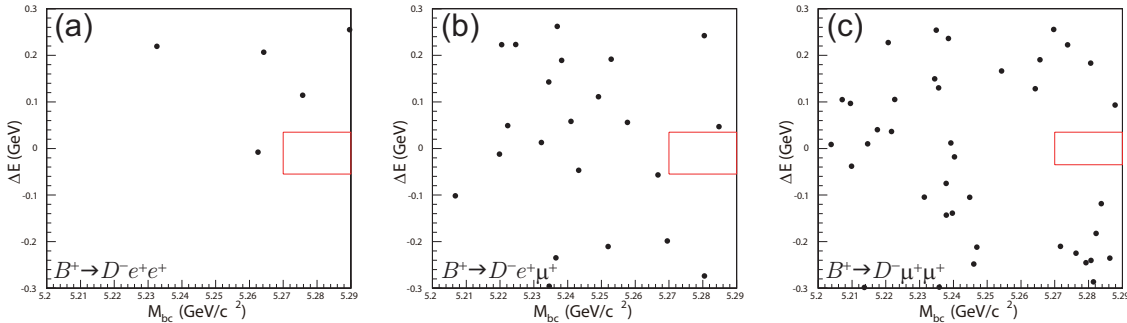


**Figure 4:** Resulting 2D plots for  $B^+ \rightarrow e^+ e^+ D^-$  (a),  $B^+ \rightarrow e^+ \mu^+ D^-$  (b) and  $B^+ \rightarrow \mu^+ \mu^+ D^-$  (c) on the  $M_{bc} - \Delta E$  plane. Here, black dots express the data and the box region is the signal one in each plot. No events are found in each mode.

## References

- [1] E. Arganda, M. J. Herrero and J. Portoles, JHEP **0806**, 079 (2008).
- [2] G. J. Feldman and R. D. Cousins, Phys. Rev. D **57**, 3873 (1998).
- [3] G. Cvetic, C. Dib, S. K. Kang and C. S. Kim, Phys. Rev. D **82**, 053010 (2010).